Geophys. J. Int. (1989) **99**, 81–90

Seismic wave resonances in 3-D sedimentary basins

J. A. Rial

MacCarthy Geophysical Observatory, Geology Department, CB No. 3315, The University of North Carolina at Chapel Hill, NC 27599-3315, USA

Accepted 1989 April 6. Received 1989 April 6; in original form 1988 August 23.

SUMMARY

The resonant eigenfrequencies of three-dimensional models of sedimentary basins are calculated through the use of high-frequency asymptotics. The results are valid for the areas near the geometrical centre of the basin, where the thickness of sediments is greatest. By analogy with the theory of electromagnetic resonators it is shown that the modes of oscillation of trapped seismic waves can be easily computed from simple formulas that relate the geometry of the basin to the type of resonant mode and to the eigenfrequencies. All results are approximations based on WKB solutions to the wave equation whose phase function satisfy resonant or 'quantum' conditions inside the basin. Comparison with published numerical data indicates that the analytical approach here described may be of more general application than the empirical formulations that have been proposed previously for two-dimensional basins.

Key words: resonant eigenfrequencies, sedimentary basins, seismic waves

1 INTRODUCTION

Estimating earthquake-induced ground motions on the surface of sediment-filled basins is an important aspect of the earthquake hazard reduction effort and a fundamental problem in seismic wave propagation. The destructive Mexican earthquake of 1985 is a sharp reminder of how little is known about the effects of three-dimensional geological structures on incident seismic waves. Data from the Mexican event strongly suggest resonance of the underlying sedimentary basin as a major cause of the heavy damage suffered by the structures (Anderson *et al.* 1986).

To solve the wave propagation problem most relevant to resonance means to be able to accurately compute the seismic wavefield after it has interacted with full 3-D media for a reasonable long time. No complete analytical solution is possible for broadband signals and/or arbitrary geometries. Solutions based upon large-scale numerical wave solvers do not provide the physical insight and generality obtainable with analytical methods, albeit being dependent on the efficient elimination of late-arriving reflections from nonphysical boundaries. After careful scrutiny, it seems that a simplified analytical approach based on wave asymptotics (high frequency) and geometrical optics (infinite frequency) is a possible alternative that results in useful answers. Such is the approach reported here.

This paper presents some theoretical results that allow easy calculation of high frequency resonant modes for simple geometrical models of 3-D sedimentary basins. Part of the motivation to undertake this study comes from a paper by Keller & Rubinow (1960), who show what types of resonant oscillations may appear inside smooth domains, even in those in which the wave equation is not separable. The results presented below are however derived from the theory of electromagnetic resonators (Weinstein 1969). Throughout his book Weinstein (who claims to have developed his theory independently of Keller & Rubinow's results) provides explicit analytical solutions for resonators of diverse geometries. Some of these have been generalized here and adapted to the sedimentary basin problem, while others have been used directly with only minor modifications.

The mathematical approach is through the use of high-frequency asymptotics and WKB solutions of the scalar wave equation in triaxial ellipsoidal coordinates. It is shown later that the selection of this coordinate system ensures ample generality as to the basin geometries for which the results apply. Low-frequency phenomena, including mode coupling between P and S waves, are not studied. The results are valid for the areas near the geometrical centre of the basin, where the thickness of sediments is greatest. The resulting analytical expressions are easy to evaluate numerically and provide a simple means to estimate the fundamental resonant frequency and overtones for P and S waves. Within the limitations imposed by the approximations made, it is found that the resonant frequencies (and overtones) depend only on the geometrical ratios H/R_i, where H is the maximum thickness of the basin and the R_i are the principal radii of curvature there. The ellipsoidal-shape constraint may be relaxed by using simple multiplicative correction terms that do not depend on the basin's shape.

Since the theory of electromagnetic resonators as developed by Weinstein (1969) may not be familiar to some

seismologists, in Section 2 I succinctly describe some results which will be needed in later sections. The expressions for the eigenfrequencies in both 2- and 3-D basins are derived in Section 3. A comparison of the theoretical results with numerically computed resonant frequencies in two dimensions is also presented there.

2 THEORY

Whether or not separability of the wave equation is possible, Keller & Rubinow's (1960) analysis predicts the existence of two types of resonant modes in a 3-D closed domain: the 'bouncing ball' modes, whose amplitudes are non-zero only inside a small volume surrounding the minimum diameter of the domain, and the 'whispering gallery' modes, with non-zero amplitudes within a thin layer lying next to the domain's boundary. Furthermore, they also point out that the bouncing ball modes are stable only along the minimum diameter of the domain, an important property that can now be easily substantiated with computer experiments. The stability of a given mode may be described in terms of sensitivity of the rays generating that mode to their initial orientation. Only when the mode is stable will all nearby ray orbits stay close to each other. If the mode is unstable, a small perturbation (as small as the computer's highest precision) in the initial orientation of the take-off angles can result in ray orbits rapidly diverging from each other even after a few bounces. This extreme sensitivity to initial conditions is nowadays recognized as typical of many dynamical systems governed by non-linear differential equations.

In this paper I shall be concerned with stable modes, linear differential equations and with the application of Weinstein's theory of resonators only. A more detailed analysis of unstable modes is the subject of a forthcoming paper.

The derivation of the solution to the Helmholtz equation inside a domain bounded by a triaxial ellipsoid can very easily be made to fit the sedimentary basin resonance problem. The theory is thoroughly described in Weinstein's book on electromagnetic resonators, so I shall only briefly describe those results of relevance to the present work. For a complete treatment the reader is referred to chapters 5 and 6 of Weinstein (1969).

In ellipsoidal coordinates the resonator is described as a triaxial ellipsoid of semi-axes $a>b>c$. The scalar Helmholtz wave equation $\Delta\mu + K^2\mu = 0$, with eigenvalues K, is assumed to correctly describe the wavefields inside the resonator. In this coordinate system the Helmholtz equation is separable, and its solution can be written as

$$\mu = X(\xi)Y(\eta)Z(\zeta) \tag{1}$$

where the functions X, Y and Z are solutions of the ordinary differential equations

$$\begin{aligned} d^2X/du^2 + K^2p(\xi)X &= 0 \\ d^2Y/dv^2 - K^2p(\eta)Y &= 0 \\ d^2Z/dw^2 + K^2p(\zeta)Z &= 0 \end{aligned} \tag{2}$$

and the following elliptical integrals have been introduced as auxiliary variables:

$$\begin{aligned} u &= \int_0^{\xi} d\Omega/[2\sqrt{D(\Omega)}] \\ v &= \int_{c^2}^{\eta} d\Omega/[2\sqrt{-D(\Omega)}] \\ w &= \int_{b^2}^{\zeta} d\Omega/[2\sqrt{D(\Omega)}]. \end{aligned} \tag{3}$$

Here $D(\Omega) = (a^2-\Omega)(b^2-\Omega)(c^2-\Omega)$; and $p(\Omega) = (\Omega - \Omega_1)(\Omega-\Omega_2)$. Ω_1 and Ω_2 are unknown parameters that determine the locations of the turning point surfaces or modal caustics of a given mode. This is clear since the zeroes of $p(\Omega)$ determine whether the solutions to each of equations (2) are oscillatory or exponentially decaying. Explicit ranges of existence for the caustic surfaces of each mode are obtained by noting that the polynomial $p(\Omega)$ must be real and that both Ω_1 and Ω_2 need to be real in order for (2) to have acceptable solutions. Weinstein (1969, p. 188) shows that there exist four independent sets of real values of the pairs Ω_1, Ω_2 in the interval $0<\Omega<a^2$, each of which determine the geometry of the modal caustics. These in turn confine the oscillations in four differently shaped volumes, two pertaining to the bouncing ball modes and two to the whispering gallery modes. Specifically, any mode in a triaxial ellipsoid belongs to one of the four types defined by the following inequalities:

$$\begin{aligned} &\text{I. } c^2<\Omega_1<\Omega_2<b^2 \\ &\text{II. } c^2<\Omega_1<b^2<\Omega_2<a^2 \\ &\text{III. } 0<\Omega_1<c^2<\Omega_2<b^2 \\ &\text{IV. } 0<\Omega_1<c^2;\ b^2<\Omega_2<a^2. \end{aligned} \tag{4}$$

Modes I and II are the bouncing ball modes, and the caustic surfaces confining the ray system are two hyperboloids of one sheet (mode I) and hyperboloids of one and two sheets (mode II). Modes III and IV are the whispering gallery modes, with caustic surfaces formed by an ellipsoid and a hyperboloid of one sheet, and an ellipsoid and hyperboloid of two sheets respectively. Explicit equations for the caustic surfaces of each mode are obtained by substituting the limiting values of Ω given in (4) into the relation

$$x^2/(a^2-\Omega) + y^2/(b^2-\Omega) + z^2/(c^2-\Omega) = 1 \tag{5}$$

which defines a one-parameter family of coordinate surfaces in the ellipsoidal system. The oscillating part of the WKB solutions to the reduced wave equation occur within the shaded volumes shown in Fig. 1. Outside these volumes the solutions decay exponentially with distance from the confining caustic surfaces. In this paper I shall be concerned with modes I and II only, the bouncing ball modes.

A sedimentary basin may be regarded as one-half of an ellipsoidal resonator. The seismic waves inside can be visualized as going through an inhomogeneous waveguide. Since the distance between the reflecting surfaces (the free surface and the bottom of the basin) is greatest at the centre and decreases towards the edges, some modes are locked-in in the central part of the basin and do not propagate horizontally. Around the locked modes caustics are formed where the bouncing rays turn around in their outgoing paths to become incoming rays. The rays describe orbits around

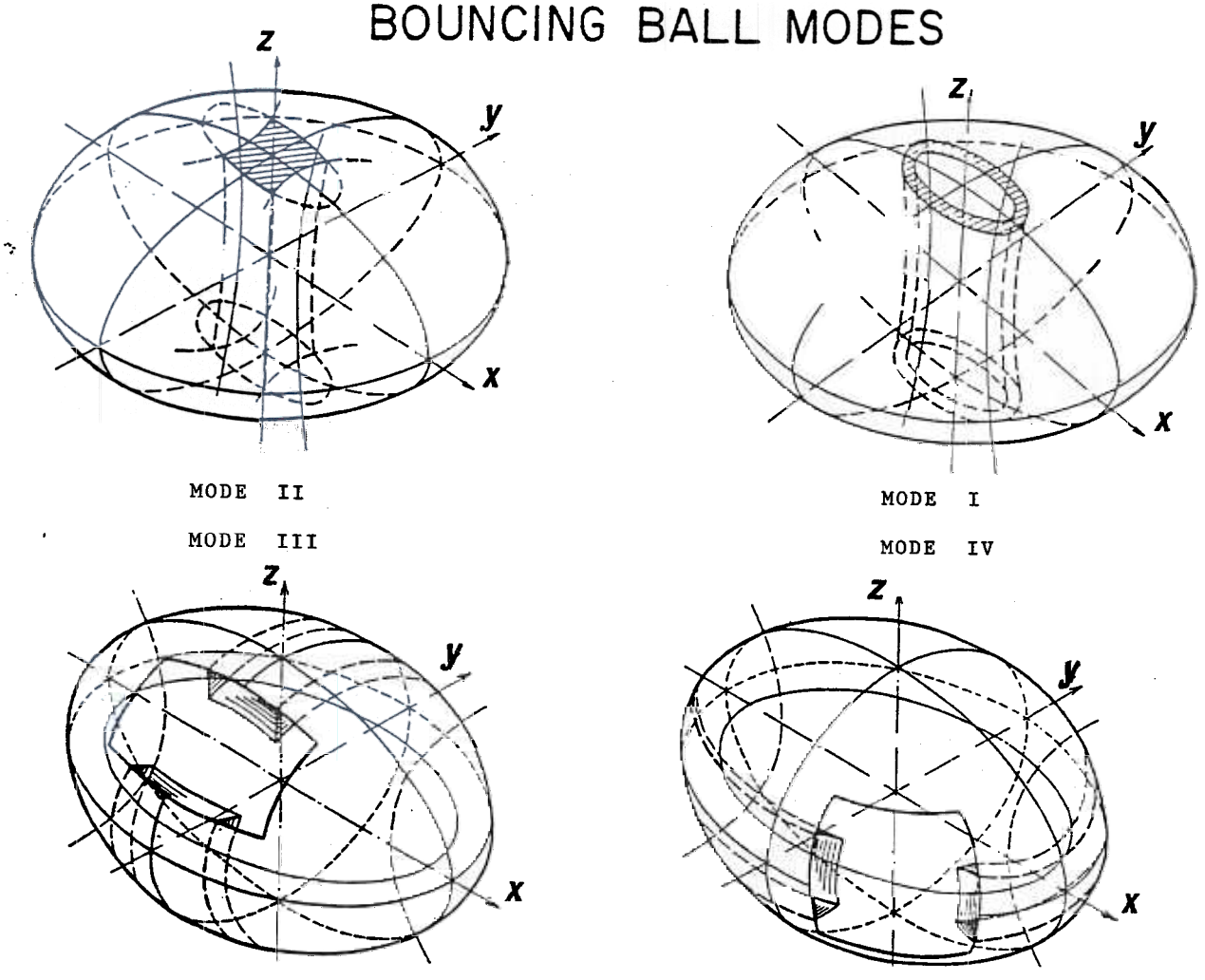

the centre of the basin in a manner fully analogous to the motions of a point mass (or charge) in an ellipsoidal potential field. It is then not surprising that in order to determine the eigenfrequencies of oscillation in a resonator one must use equations (6) below, which are analogues of the quantization rules of electron orbits in Bohr's old quantum mechanics. Although most commonly used in quantum mechanical problems, these rules are also applicable to, for instance, seismological studies of asymptotic normal modes in a lateral heterogeneous model of the earth (Dahlen & Henson 1985). The interested reader is also referred to Keller (1985) for a review of methods and applications of semi-classical mechanics that may be of use in seismic wave propagation.

3 EIGENVALUES AND RESONANT FREQUENCIES

Weinstein (1969, ch. 6) gives the explicit form of the three resonance conditions (also popularly known as Bohr–Sommerfeld quantum conditions) for the wavenumber K in the triaxial ellipsoidal resonator of semiaxes $a > b > c$:

$$K\left(\int_0^{c^2} P(\Omega)\, d\Omega\right) = \pi \mathbf{l}$$

$$K\left(\int_{\Omega_1}^{\Omega_2} P(\Omega)\, d\Omega\right) = 2\pi(\mathbf{m} + 1/2)$$

$$K\left(\int_{b^2}^{a^2} P(\Omega)\, d\Omega\right) = \pi \mathbf{n} \qquad \mathbf{l}, \mathbf{m}, \mathbf{n} = 0, 1, 2, 3, \cdots \qquad (6c)$$

for mode I. Similar equations apply for modes II–IV. Conditions (6) are standard in form and easily derived once the WKB solution is known for each of the three coordinate-dependent separable functions X, Y and Z of (1). Each of the integrals in (6) is taken over the domains of the ellipsoidal variables where the mode is defined by the inequalities given in (4). Equations (6) illustrate the fact that for any given ray to constructively interfere, the accumulated phase along a closed trajectory (including

phase jumps at caustics) must be an integer multiple of the wavelength. The function $P(\Omega)$ is given by the expression

$$P(\Omega) = \sqrt{[p(\Omega)/D(\Omega)]}. \quad (7)$$

The integers $\mathbf{l}, \mathbf{m}, \mathbf{n}$ define the particular eigenvalue or eigenfunction. Weinstein's theory requires $\mathbf{l} \gg 1$, but Keller & Rubinow (1960) found numerically that the approximation is good even for small $\mathbf{l}$. Once the integrations are performed the resulting equations can be solved for K and for the location of the caustics. The integrals in (6) can be evaluated in several ways depending on the nature of the problem and on the approximation required. In this paper the objective is to apply these results to obtain the high frequency eigenvalues of one-half ellipsoids (or sedimentary basins) with the adequate (seismic) boundary conditions. This is done next.

3.1 Mode I

Integration of (6) is straightforward. After a little algebra one gets from (6a):

$$2Kc(a/b) - K[(t_1 - t_2)/\sqrt{(a^2 - b^2)}]\mathbf{F}(\emptyset, s_1) + K[(a^2 + b^2 - 2c^2)/\sqrt{(a^2 - c^2)}]\mathbf{F}(\emptyset, s_1) - 2K\sqrt{(a^2 - c^2)}\mathbf{E}(\emptyset, s_1) = \pi\mathbf{l}. \quad (8a)$$

From (6b):

$$K/\sqrt{(b^2 - c^2)}[t_2(t_1 + t_2)/\sqrt{(t_3 t_4)}\,\Pi(w_1, s_2) - \sqrt{(t_3 t_4)}\,\mathbf{E}(s_2) - t_2\sqrt{(t_3/t_4)}\,\mathbf{K}(s_2)] = 2\pi(\mathbf{m} + 1/2). \quad (8b)$$

From (6c):

$$K/\sqrt{(a^2 - c^2)}[t_2(t_1 + t_2)/\sqrt{(t_3 t_4)}\,\Pi(w_2, s_2) + \sqrt{(t_3 t_4)}\,\mathbf{E}(s_2) - t_2\sqrt{(t_4/t_3)}\,\mathbf{K}(s_2)] = \pi\mathbf{n} \quad (8c)$$

where $\mathbf{F}(\emptyset, s)$ and $\mathbf{E}(\emptyset, s)$ and $\Pi(w, s)$ are the incomplete elliptical integrals of the first, the second and the third kind respectively, and $\mathbf{E}(s)$ and $\mathbf{K}(s)$ are the complete elliptical integrals of the second and third kinds (see for instance Byrd & Friedman 1971).

The variables and parameters are given by the following expressions:

$$t_1 = a^2 - \Omega_1 \quad \emptyset = \arcsin(c/b) \quad s_1 = (a^2 - b^2)/(a^2 - c^2)$$
$$t_2 = b^2 - \Omega_2 \quad w_1 = \sqrt{[(t_3 - t_2)/t_3]} \quad s_2 = w_1 w_2$$
$$t_3 = b^2 - \Omega_1 \quad w_2 = \sqrt{[(t_1 - t_3)/t_4)]}$$
$$t_4 = a^2 - \Omega_2.$$

From (8b) and (8c) and by using the addition formulae for elliptic integrals, it is easy to show that

$$K(t_1 + t_2) = 4(\mathbf{m} + 1/2)\sqrt{(b^2 - c^2)} + 2\mathbf{n}\sqrt{(a^2 - c^2)}$$

from which the wavenumber K can be solved for to give the following resonance condition in the ellipsoidal resonator of semiaxes a, b, c.

$$2Kc(a/b) + K[(a^2 + b^2 - 2c^2)/\sqrt{(a^2 - c^2)}]\mathbf{F}(\emptyset, s_1) - 2K\sqrt{(a^2 - c^2)}\mathbf{E}(\emptyset, s_1) = \pi\mathbf{l} + [2(2\mathbf{m} + 1)(b^2 - c^2)/\sqrt{(a^2 - c^2)} + 2\mathbf{n}]\mathbf{F}(\emptyset, s_1). \quad (9)$$

Equations (8) and (9) are valid for eigenvalues K within an ellipsoidal domain subjected to homogeneous boundary conditions, i.e. $\mu(x, y, z)$ or its normal derivatives must vanish on the surface of the ellipsoid.

An illustration of the ray trajectories associated with the modes is given by the ray tracings of Figs 2 and 3 which show the horizontal projections of the rays as they bounce off the free surface of basins formed by half ellipsoids. Figure 2 shows how the bouncing ball mode I is readily developed after a few hundred bounces of a single ray (or equivalently, after a few bounces of several hundred rays). Confining the motion are the caustic surfaces, at which the rays turn

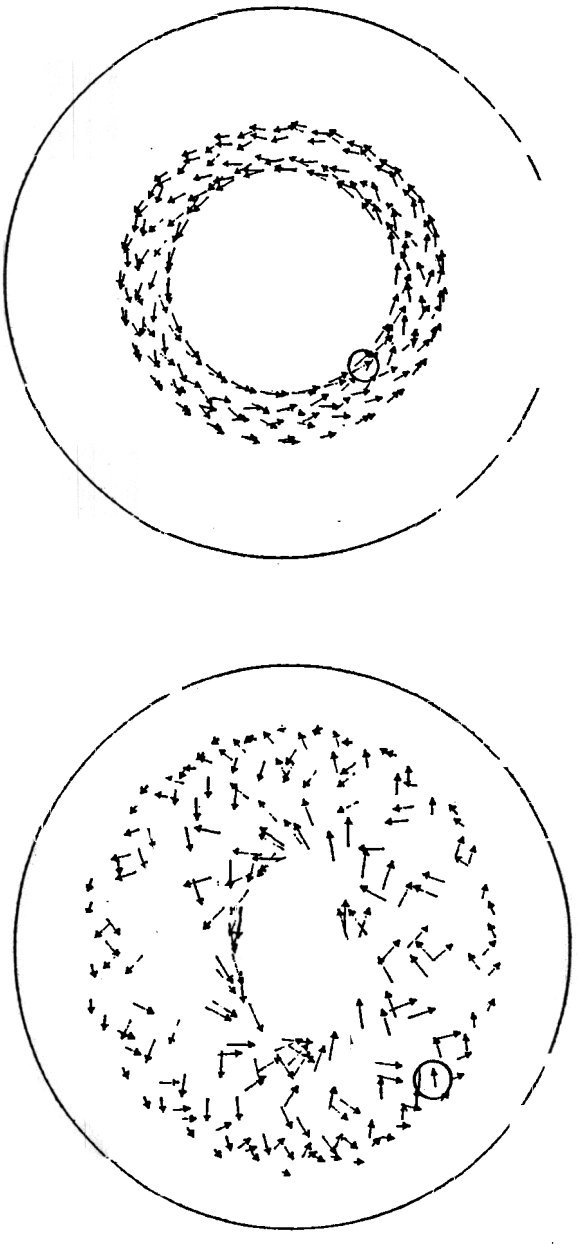

Figure 2. Radially symmetric basin (top) showing the development of mode I and in a slightly elliptical basin (bottom). In both figures the arrows represent the horizontal projection of a unit vector directed along the ray just after reflection from the free surface. An initial ray (marked by a circle) is allowed to bounce 200 times inside the basin. The outline curves are selected contour lines at arbitrary depths below the surface.

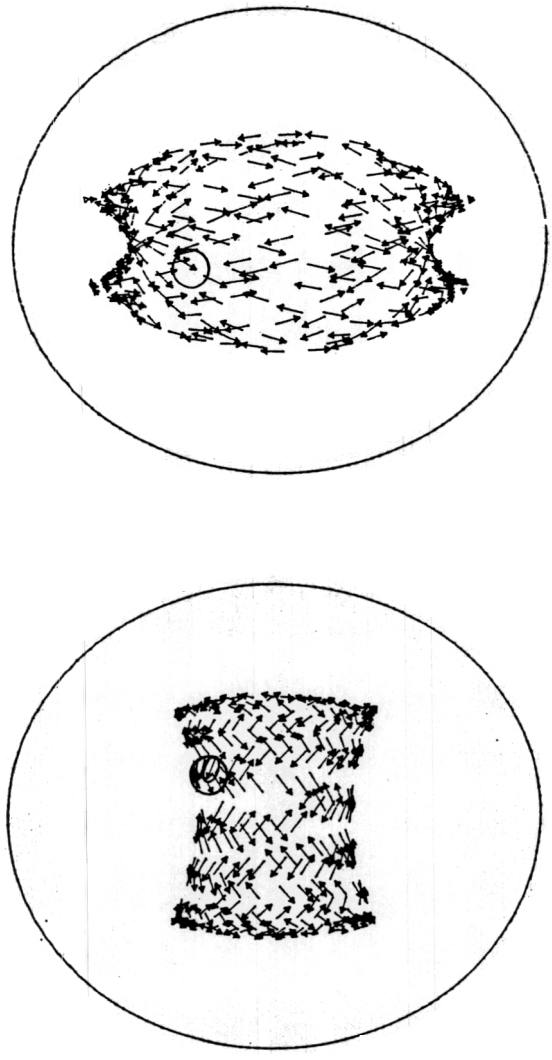

Figure 3. As in Fig. 2, but for basins of increased ellipticity, in which mode II (top and bottom) is more readily excited than mode I.

around in their 3-D path. Outside of the ray-filled space the amplitudes of the waves decay exponentially with distance from the caustic surfaces, i.e. the eigenoscillations become isolated from other parts of the basin, remaining horizontally trapped by the caustics for the duration of the oscillations. It can be shown that similar patterns are observed for basins formed by Gaussian, cosine or other similar (non-separable) bounding surfaces as long as the oscillations are stable.

The derivation of (8) assumes that $d\Omega/\Omega_1 \ll 1$, where $d\Omega = \Omega_2 - \Omega_1$. This is equivalent to requiring that the rays stay in the neighbourhood of the ellipsoid's vertical axis (semi-axis c) and away from its edges (paraxial approximation). A result arrived at by Weinstein (1969, ch. 6) is easily obtained from (8) by setting $a = b$ in (9), i.e.:

$$2Kc = \pi\mathbf{l} + 2(2\mathbf{m} + \mathbf{n} + 1)\arcsin(c/a)$$

which can also be written as

$$2Kc = \pi\mathbf{l} + (2\mathbf{m} + \mathbf{n} + 1)\arccos[1 - 2(c/a)^2] \qquad (10)$$

with $\mathbf{l}, \mathbf{m}, \mathbf{n} = 0, 1, 2, 3, \cdots$, for an oblate ellipsoid.

For the case in which the two opposite reflectors have different curvature, i.e. for an asymmetric resonator, equation (10) must be changed to (Weinstein 1969);

$$2d/\lambda = \mathbf{l} + (1/\pi)(2\mathbf{m} + \mathbf{n} + 1) \times \arccos\{\sqrt{[(1 - d/r')(1 - d/r'')]}\} \qquad (11)$$

where r' and r'' are the radii of curvature of the two opposing reflecting surfaces of the resonator; $d = 2c$, and $K = 2\pi/\lambda$, where λ is the wavelength. If now r'' is let to approach infinity, equation (11) becomes

$$2d/\lambda = \mathbf{l} + 1/(2\pi)(2\mathbf{m} + \mathbf{n} + 1)\arccos(1 - 2d/r') \qquad (12)$$

where d is the distance between the flat and the curved reflectors, at the centre of the one-half ellipsoid.

3.2 Mode II

In this case, the appropriate expression for the eigenvalues is again obtained from equations (6) with the rhs's slightly changed, as in Weinstein (1969), to account for the mode's geometry. The inequalities II of (4) determine the integration intervals. The integrations give, after some algebra:

$$2Kc = \pi\mathbf{l} + (2\mathbf{m} + 1)\beta_1 + (2\mathbf{n} + 1)\beta_2 \qquad (13)$$

with

$$\beta_1 = \arcsin\sqrt{(c/R_1)} \qquad 0 \le \beta_1 \le \pi$$

$$\beta_2 = \arcsin\sqrt{(c/R_2)} \qquad 0 \le \beta_2 \le \pi$$

R_1 and R_2 are the principal radii of curvature of the ellipsoid at the point $x = y = 0$. For equation (8) to apply the ellipsoid must be such that $a \neq b$. It should be obvious from the inequalities (4) and from (13) that if the ellipsoid is axially symmetric ($a = b$), mode II does not exist. This reveals the importance of attacking the full 3-D problem, which requires the use of ellipsoidal coordinates. Mode II (Fig. 3) cannot be known to exist if the ellipsoid's geometry is constrained by numerical or computational convenience to be axially symmetric. It can also be shown that in a non-axisymmetric ellipsoid, mode I will be excited by rays whose initial direction inside the ellipsoid do not cross any of the interfocal lines, whereas mode II is excited by those rays whose initial direction crosses the interfocal lines. This is an elementary geometric property easy to confirm with ray-tracing, as can be observed in Figs 2 and 3. It implies that mode II will be more readily excited the more elongated the ellipsoidal (or the basin) is, and that axisymmetric basins will resonate only in mode I of the bouncing ball modes.

Similar to the previous case, in order to obtain an expression for the one-half ellipsoid, equation (13) can be written:

$$Kd = \pi\mathbf{l} + (\mathbf{m} + 1/2)\arccos\sqrt{[(1 - d/R_1)(1 - d/R_1')]} + (\mathbf{n} + 1/2)\arccos\sqrt{[(1 - d/R_2)(1 - d/R_2')]} \qquad (14)$$

where d is, as before, the distance between the upper and lower reflectors. R_1' and R_2' are thus the principal radii of curvature of the upper reflector at $x = y = 0$. Letting R_1' and

R_2' go to infinity (14) becomes:

$$2d/\lambda = \mathbf{l} + (1/2\pi)[(\mathbf{m}+1/2)\arccos(1-2d/R_1) + (\mathbf{n}+1/2)\arccos(1-2d/R_2)]. \quad (15)$$

3.3 Seismological applications

So long as the previous results apply to high frequency waves (or wavelengths short compared with the dimensions of the basin) and to geometrical rays bouncing back and forth within an ellipsoidal domain, we may modify expressions (12) and (15) to obtain the corresponding results for a sedimentary basin shaped as half an ellipsoid with semi-axes a, b and c. The a, b plane is the Earth's free surface where stress-free boundary conditions are assumed. The semi-axis $c = H$, is the maximum depth of the basin. For simplicity, the seismic impedance contrast between the (uniform, elastic and isotropic) sediment and the underlying rock is assumed high enough so that the lower boundary can be considered rigid, and thus the waves may be fully trapped by the basin. This idealized model may be called a geological resonator.

The oscillations are assumed to be closely packed near the least diameter of the ellipsoid, so angles of incidence/reflection at the top and bottom boundaries must be small.

SH-wave high frequency resonant eigenvalues in a solid or P-wave modes in a fluid may be obtained with acceptable accuracy. This is because the foregoing theory is based on a scalar description of wave interaction (the vector wave equation is not separable in ellipsoidal coordinates). In 3-D solids equations (12) and (15) may also be properly used to estimate resonant frequencies as long as high frequency, distinctively polarized oscillations of P and S waves occur independently of each other. In fact, it is shown below that it is possible to evaluate the resonant frequencies associated with P, SV and SH oscillations in a 2-D model of a sedimentary basin through the use of (15).

A useful result in 3-D can be obtained from (12) for an axisymmetric sedimentary basin with $a = b > c = H$

$$f = f_0[(2\mathbf{l}+1) + (1/\pi)(2\mathbf{m}+\mathbf{n}+1)\arccos(1-2H/R)] \quad \mathbf{l}, \mathbf{m}, \mathbf{n} = 0, 1, 2, 3, \ldots, \quad (16)$$

where f are the eigenfrequencies of resonance in cycles per second, $f_0 = v/4H$ is the resonant frequency (fundamental mode, $\mathbf{l} = 0$) for the flat-layered case, with v being the wavespeed in the sediments. R is the radius of curvature of the basin at its deepest point. The factor $(2\mathbf{l}+1)$ instead of $2\mathbf{l}$ in (16) is used since the total phase shift due to top (free surface) and bottom (rigid boundary) reflections for near normal incidence is $-\pi$ for S or P waves and near-normal incidence. It is worth noting that, according to (16), $f = 2f_0$ for a hemispheric basin's $(H = R)$ fundamental mode $(\mathbf{l} = \mathbf{m} = \mathbf{n} = 0)$.

Also note that $f = f_0(2\mathbf{l}+1)$ $\mathbf{l} = 0, 1, 2, 3, \ldots,$ as R approaches infinity, i.e. the expected 1-D result for wave eigenfrequencies in a flat layer overlying a rigid halfspace.

Similarly from (15) one can easily obtain, for $a > b > H$ (mode II):

$$f = f_0[2\mathbf{l} + (1/\pi)(\mathbf{m}+1/2)\beta_1 + (1/\pi)(\mathbf{n}+1/2)\beta_2] \quad (17)$$

with

$$\beta_1 = \arccos(1-2H/R_1) \qquad 0 \le \beta_1 \le \pi$$
$$\beta_2 = \arccos(1-2H/R_2) \qquad 0 \le \beta_2 \le \pi$$
$$\beta_1 \neq \beta_2 \quad \text{and} \quad \mathbf{l}, \mathbf{m}, \mathbf{n} = 0, 1, 2, 3, \cdots.$$

R_1 and R_2 are the principal radii of curvature at the deepest point of the basin, $R_1 = a^2/H$ and $R_2 = b^2/H$, for a triaxial ellipsoid.

3.4 Comparison with numerical results for a 2-D basin

From equation (17) by letting the long semi-axis a go to infinity one can obtain the eigenfrequencies for a 2-D elliptic basin as:

$$f = f_0[(2\mathbf{l}+1) + (1/\pi)(\mathbf{q}+1/2)\arccos(1-2H/R)] \quad (18)$$

with $\mathbf{l}, \mathbf{q} = 0, 1, 2, 3, \ldots,$ and $R = b^2/H$, with b and H being the horizontal and vertical semi-axes of the elliptical basin respectively. To obtain (18) a factor of $-\pi$ has been added on the left-hand side of (17) to account for the fact that one of the reflecting surfaces is now traction-free. This same phase shift is applicable to P, SV and SH waves as long as near-normal incidence is assumed. I have selected published numerical data by Bard & Bouchon (1985) to compare with equation (18). The data (open triangles in Fig. 4) refer to a basin with a cosine shape. The calculated f/f_0 is plotted as a function of H/L, where L is the cosine's semiwavelength.

Equation (18) can not be directly applied to a cosine-shaped basin. If however we consider an elliptical basin with the same maximum depth, and the same radius of curvature at its deepest point, (18) can be used as long as it is corrected for the difference in surface areas of the two domains. This correction amounts to changing (18) into

$$f = f_0[(2\mathbf{l}+1) + (1/\pi)(S_e/s_c)^{1/2}(\mathbf{q}+1/2)\arccos(1-2H/R)] \quad (19)$$

where S_e and S_c are the surface areas of the elliptical and the cosine-shaped basins respectively. This correction is based on the well-known fact that asymptotically,

$$K_n \sim (4\pi n/S)^{1/2} \quad (20)$$

where K_n is the nth eigenvalue of the reduced wave equation $\Delta\mu + K^2\mu = 0$ and S is the surface area of the domain. Here it is important to recall that asymptotically the values of K depend only on the size of the domain and are independent of the domain's shape and the boundary conditions (Courant & Hilbert 1953, vol. I, ch. 6).

Figs 4(a) and (b) show the curves generated by equations (18) and (19) respectively for P, SH and SV waves. The 2-D resonances may be classified in two categories: the antiplane shear (SH) and the in-plane shear (SV) and bulk (P) modes. It is easy to show that in the limit of a horizontal layer over a rigid halfspace, the 1-D resonant conditions (in near normal incidence) for SH waves are $f/f_0 = 2p+1$, whereas for P and SV waves are $f/f_0 = 2p$ (the value of f_0 being the appropriate in each case), p being any positive integer. Thence the 2-D resonant modes must also be separated into the same two categories with respect to the horizontal oscillations, namely; symmetric such that in (19) $\mathbf{q} = 2p$ for P and SV waves (the in-plane modes), and antisymmetric

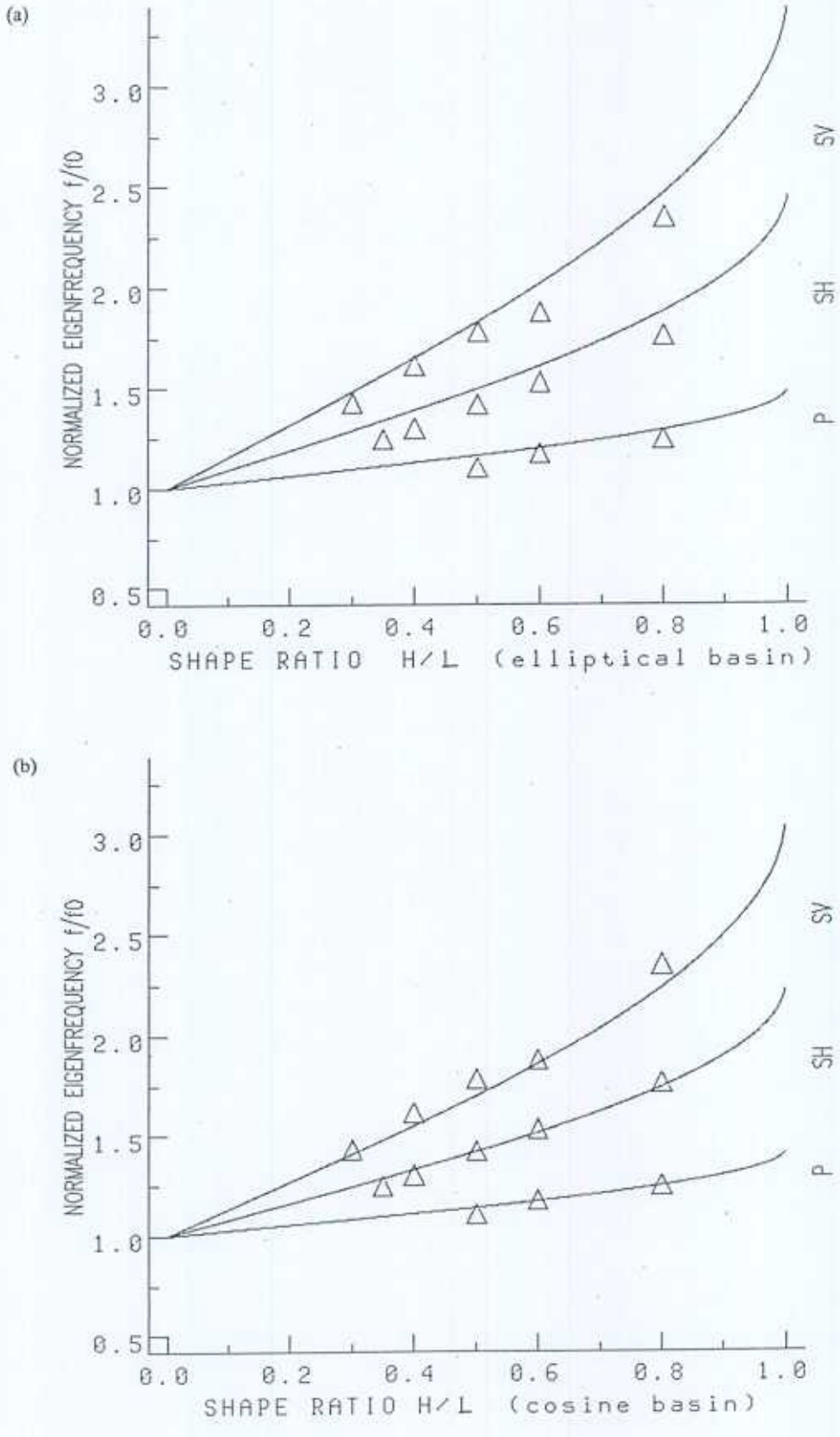

Figure 4. Comparison of numerical results reported by Bard & Bouchon (1985) (open triangles) with values obtained from equation (18) for an elliptical, 2-D basin with the same maximum thickness and central curvature as Bard & Bouchon's cosine basin (a), and for a simulated cosine basin (b), i.e. with values obtained from equation (19). In both cases the shape ratio used in equations (18) and (19) is the ratio between the vertical and horizontal semi-axes of the ellipse. All curves are for the fundamental radial mode ($l = 0$). See text for details.

such that $\mathbf{q} = 2p + 1$, for SH waves (the antiplane mode). Thence, in order to obtain eigenvalues compatible with the numerical results of Fig. 4, equation (19) must be used with $\mathbf{q} = 0$ and $\mathbf{q} = 2$ for P and SV waves respectively, and $\mathbf{q} = 1$ for SH waves. For all three waves the vertical resonance parameter $\mathbf{l}$ must obviously be zero. Furthermore, if (19) above is compared with Bard & Bouchon's empirical relations, it is seen that both give nearly the same results for small H/L as long as their integers m and n (Bard & Bouchon 1985, see pp. 535, 536) have respectively the same values of $\mathbf{l}$ and $\mathbf{q}$ above for P, SV and SH.

Since the empirical formulae proposed by Bard & Bouchon are based on results for a rectangular inclusion embedded in a rigid half-space, it is not surprising that their predictions are invalid for curved-boundary basins, especially as the curvature increases. Equation (19) in contrast, seems to account correctly for the curvature effect.

The comparison with the data indicates that (19) may accurately predict the eigenfunctions of a cosine-shaped basin as long as the shape ratio used in plotting is H/b, rather than H/L. Also, (18) seems to correctly give the eigenfunctions for elliptical basins and thus the empirical formulae proposed by Bard & Bouchon (1985) do not appear to be necessary.

For 3-D domains, a similar rule to (20) is

$$K_n \sim [6\pi n/V]^{1/3} \tag{21}$$

where V is the domain's volume.

4 DISCUSSION

4.1 Strong ground resonances

Most urban areas are built on sediment-filled, bowl-shaped basins. Despite this fact, the engineer's analyses of ground response relies heavily on 1-D formulae. These may sometimes be helpful, but it should be obvious that the predictions that can be made with a 1-D theory may be limited in scope. In this regard it is worth discussing the 1985 Michoacan (Mexico) earthquake, as recorded on Mexico City's sedimentary basin. This destructive earthquake induced long-lasting, resonant accelerations that exceeded the predicted design spectrum at several locations within the basin. At station SCT, for instance, ground accelerations reached spectral amplitudes four times greater than those predicted by the city's 1977 Building Code. These were excessive levels of ground shaking for many buildings, some of which collapsed or suffered major damage. Most of the damage occurred within the old lake area of the city, where the soil is composed of water-saturated soft clays, 35–50 m thick, overlying compact sands and gravels (Anderson *et al.* 1986; Romo & Seed, 1987).

One important aspect of the study of this and previous damage patterns in Mexico City is that there exist different opinions as to what role the soft clay layer played in the excitation of the observed resonant frequencies, and as to how the geometry of the basin influenced the ground motions. For instance, one of the best studied and most characteristic records of the oscillations was obtained at station SCT. Here, accelerations occurred with a spectrum strongly peaked at a frequency (~0.5 Hz) twice as high as that estimated for the city by Herrera, Rosenblueth & Rascon (1965) with the formula

$$f_{\mathbf{n}} = (v/4H)(2\mathbf{n} + 1) \qquad \mathbf{n} = 0, 1, 2, 3, \ldots, \tag{22}$$

for an average stratigraphic section in Mexico City. A commonly accepted argument explains this discrepancy by assuming that the oscillations within the basin are actually confined to the uppermost 35–50 m of the very soft clays (shear-wave velocity 70–100 m s^{-1}), rather than to the full thickness (~500 m) of the basin. In fact, acceleration response spectra calculated by Romo & Seed (1987) from observed accelerograms have central frequencies of 0.26, 0.36 and 0.5 Hz at lake-bed stations CAO, CAF and SCT respectively. The sediment depths are 58 m at CAO, 45 m under CAF, and around 37 m under SCT; the shear wave velocities vary from an average 70 m s^{-1} at CAO and CAF, to an average 77 m s^{-1} under SCT. Thus, within the possible uncertainties in the parameters, equation (22) with $\mathbf{n} = 0$ gives frequencies in close agreement with the observed, especially at SCT. Romo & Seed (1987) find in these results strong justification for the use of 1-D analyses of the ground response.

However, other investigators point out that Mexico City's basin geometry is such that waves can be trapped horizontally, interfere and produce localized amplification of ground shaking that can strongly modify the local ground shaking. These are 2- or 3-D aspects of the dynamic soil response totally overlooked by 1-D analyses (Whitman 1987). As to the assumption that most of the oscillations are confined and controlled by the response of the soft clay layer, some investigators have expressed doubt that surface or body waves 2 s in period can be influenced by a 50 m thick layer, no matter how soft the clay may be (J. Johnson 1986, USGS Open File Report 86-401, p. 109).

Whether or not those objections can be substantiated, it is worth noting that the values of the observed resonant frequencies can just as well be obtained from equation (16) that includes the effects of the basin's curvatures, as follows: let the average resonant frequency for a flat section of the basin be 0.25 Hz, i.e. close to that observed at CAO which is also close to Herrera *et al.* (1965) horizontal layer average value of 0.22 Hz and assume that under SCT the curvature of the interface is such that it is justifiable to set $H \sim R$ in (16). This assumption means that the basin's boundary under SCT must be nearly hemispherical, and thus that a strongly focused, highly monochromatic mode I resonance could develop there. Under these conditions equation (16) gives the observed resonant frequency at SCT (0.5 Hz). Note that many combinations of sediment depth and shear wave velocity such that $v/4H = 0.25$ Hz are possible, since the individual values of v or H are left undetermined. The observed resonant frequencies at the other two stations can equally well be explained by a suitable combination of sediment thickness, shear wave velocity and basin curvature. Qualitatively at least, a hemispherical basin boundary at some depth under SCT could explain why the observed peak spectral acceleration at SCT is so much greater, and the frequency band narrower, than at CAO or CAF, an important characteristic of the spectra not accounted for in Romo & Seed's numerical simulations. Since all the formulae in this paper were derived using a WKB approximation, it is justifiable to use (16) or (17) to

determine a local resonant frequency that depends only on the curvatures of the basin under the site, and not on the overall shape of the basin.

Unfortunately, the low number of recorded accelerograms within the Mexico City basin prevent a more detailed study. Also, the available subsurface maps are not detailed enough to either support or rule out the presence of the assumed basin's curvatures under the stations.

It may still be argued that the local resonant frequencies of the ground in a sedimentary basin such as Mexico City's can, and in fact have been accurately predicted with the 1-D formula (22). The theoretical results presented in this paper suggest that (22) is indeed a good approximation, unless the effects of the curvature of the basin's boundary become important. As exemplified in Fig. 4(b), even in 2-D domains these effects can be appreciable. Equations (16) and (17) account for the resulting variation in resonant frequency when such effects are present, whereas (22) does not.

A satisfactory explanation of the Mexican data discussed above will probably have to wait for more analyses and data. On the other hand, it seems clear to researchers that most of the damage in Mexico City occurred because the natural frequency of buildings five to 20 storeys high coincided or nearly coincided with the predominant frequency of ground motion, a phenomenon that has been called double resonance by Rosenblueth (1986). In this regard, the US seismological and engineering communities have strongly recommended that microzonation maps of the US should clearly specify that siting of high-rise structures having resonant periods equal or nearly equal to that of the predominant period of ground shaking of the site should be avoided (Tinsley & Rogers 1986). Since at the same time Gulliver (1986) has pointed out that predicted-intensity maps currently in use do not account for sedimentary basin resonance effects, the implication is clear that there is a need for a theoretical-experimental methodology that can accurately compute resonant frequencies in full 3-D domains. This would allow accurate prediction of potential double resonance, especially in sediment-filled basins where the effects of lateral confinement generally translate into long-lasting, highly amplified ground shaking.

It is hoped that the results presented in this paper may be useful, although the limitations imposed on the general validity of equations (9) and (13) by the use of asymptotics, paraxiality and a description in terms of the scalar wave equation, are probably severe. Nevertheless, the comparison of the results obtained here with the numerical data of Bard & Bouchon (1985) suggests that equations (9) and (13) may in general give acceptable values of the eigenfrequencies in the 3-D case as well. An interesting implication of these equations is that the presence of a sedimentary basin just increases the resonant frequencies of the ground with respect to those of a horizontally layered section, and that such an increase can be as large as a factor of two.

4.2 Stability of the oscillations

In 3-D space it is more realistic to simulate sedimentary basins with cosine or Gaussian functions than with half-ellipsoids, but near the centre of the basin the local principal curvatures of Gaussians or cosinoids do not differ much from those of an ellipsoid. Thus the asymptotic values that can be obtained with the use of (9), (13) and (21) should be applicable to all those shapes. It should be clear however that the foregoing methods are based on the precept that the ray trajectories are bounded by smooth caustic surfaces, and that along those trajectories there is regular, predictable wave motion. The dynamics of seismic waves trapped within a geological resonator of arbitrary geometry is fairly more complicated than that, and includes the possibility of the existence of irregular, chaotic or non-integrable motions (Sorauf & Rial 1988; Rial & Sorauf 1987). Furthermore, an important numerical result is that in the presence of irregular motions the nodal surfaces of the eigenfunctions do not follow an orderly, geometrical pattern as in the case of stable resonances, but appear to wander randomly across the domain (see for instance Berry 1981, 1983, 1987; Helleman 1980; Lichtenberg & Lieberman, 1983, ch. 6) and the eigenvalues are not described by deterministic formulae. This is the topic of a forthcoming paper.

ACKNOWLEDGMENTS

I acknowledge comments and suggestions from Jeffrey Park and especially from an anonymous reviewer. This research has been supported by a grant from the University of North Carolina (URC). Technical assistance by Alberto Rial (Corpoven, Venezuela) is greatly appreciated.

REFERENCES

Anderson, J. G., Bodin, P., Brune, J. N., Prince, J., Singh, S. K., Quaas, R. & Onate, M., 1986. Strong ground motion from the Michoacan, Mexico, earthquake, *Science*, **233**, 1043–1048.

Bard, P. & Bouchon, M., 1985. The two-dimensional resonance of sediment-filled valleys, *Bull. seism. Soc. Am.*, **75**, 519–542.

Berry, M. V., 1981. Regularity and chaos in classical mechanics, illustrated by three deformations of a circular 'billiard', *Eur. J. Phys.*, **2**, 91–102.

Berry, M. V., 1983. Semiclassic mechanics of regular and irregular wave motion, in *Chaotic Behavior of Deterministic Systems* (Les Houches XXXVI), eds Ioos, G., Helleman, R. G. & Stora, R., North-Holland, Amsterdam.

Berry, M. V., 1987. Quantum chaology, *Proc. R. Soc. A*, **413**, 183–198.

Byrd, P. F. & Friedman, M. D., 1971. *Handbook of Elliptic Integrals for Engineers and Scientists*, 2nd edn, Springer-Verlag, New York.

Courant, R. & Hilbert, D., 1953. *Methods of Mathematical Physics*, vol. I, Interscience, New York.

Dahlen, F. & Henson, I., 1985. Asymptotic normal modes of a laterally heterogeneous earth, *J. geophys. Res.*, **90**, 12653–12681.

Gulliver, R. M., 1986. Some insights on the use of shaking intensities in earthquake loss estimation, in *Future Directions in Evaluating Earthquake Hazards in Southern California*, pp. 158–172, USGS Open File Report 86–401.

Helleman, R. H., 1980. Self-generated chaotic behavior in non-linear mechanics, in *Fundamental Problems in Statistical Mechanics*, vol. 5, pp. 165–233, ed. Cohen, E. North-Holland, Amsterdam.

Herrera, I., Rosenblueth, E. & Rascon, O., 1965. Earthquake spectrum prediction for the valley of Mexico, *Proc. 3rd World Conf. on Earth Eng.*, New Zealand, pp. 61–74.

Keller, J. B., 1985. Semiclassical mechanics, *SIAM Rev.*, **27**, 485–504.

Keller, J. B. & Rubinow, S. I., 1960. Asymptotic solution of eigenvalue problems, *Ann. Phys.*, **9**, 24–75.

Lichtenberg, A. J. & Lieberman, M. A., 1983. *Regular and Stochastic Motion*, Springer-Verlag, New York.

Rial, J. A. & Sorauf, C. M., 1987. The excitation of sedimentary basin resonances by multiple reflected seismic waves. Stable and stochastic behavior of horizontally trapped waves (abstract), *Eos, Trans. Am. geophys. Un.*, **68**, 352.

Romo, M. P. & Seed, B., 1987. Analytical modelling of dynamical soil response in the Mexico earthquake of September 19, 1985, in *The Mexico Earthquakes – 1985*, pp. 148–162, eds Cassaro, M. A. & Martinez Romero, E., ASCE, New York.

Rosenblueth, E., 1986. The Mexican earthquake: a first hand report, *Civil Engineering*, 38–40, ASCM, New York.

Sorauf, C. M. & Rial, J. A., 1988. A numerical study of caustics and polarizations of seismic waves interacting with three-dimensional geologic structures, *Appl. Num. Math.*, **4**, 71–81.

Tinsley, J. C. & Rogers, A. M., 1986. Suggested directions in earthquake shaking microzonation research, in *Future Directions in Evaluating Earthquake Hazards in Southern California*, pp. 345–354, USGS Open File Report 86–401.

Weinstein, L. A., 1969. *Open Resonators and Open Waveguides*, The Golem Press, Boulder, Colorado.

Whitman, R. V., 1987. Are the soild depositions in Mexico City unique?, in *The Mexico Earthquakes – 1985*, pp. 163–177, eds Cassaro, M. A. & Martinez Romero, E. ASCE, New York.